

DESY 75/06
March 1975



Scaling of $\sigma_{e^+e^- \rightarrow \text{Hadrons}}$ in Asymptotically Nonfree Theories

by

F. Gutbrod and W. Kerler

To be sure that your preprints are promptly included in the
HIGH ENERGY PHYSICS INDEX ,
send them to the following address (if possible by air mail) :

DESY
Bibliothek
2 Hamburg 52
Notkestieg 1
Germany

Scaling of $\sigma_{e^+e^- \rightarrow \text{hadrons}}$ in
asymptotically nonfree theories

by

F. Gutbrod and W. Kerler ⁺

Deutsches Elektronen-Synchrotron DESY, Hamburg, Germany

⁺ On leave of absence from Fachbereich Physik,
Universität Marburg, Marburg, Germany

Abstract

$\sigma_{e^+e^- \rightarrow \text{hadrons}}$ is calculated from the Dyson form of the photon self-energy. For the vertex of the elementary constituents the Nakanishi representation is used. A regularization scheme for the Nakanishi spectral function is taken from perturbation theoretic considerations. With simple assumptions about the spectral function, the renormalizability of the theory leads to the asymptotic form $\sigma_{e^+e^- \rightarrow \text{hadrons}} \sim \text{const}/s$. The constant depends on the anomalous dimension of the propagator. The transition to the asymptotic region occurs rather slowly. No jets are expected in the final state and the elementary constituents need not appear in the final state to an appreciable fraction.

I. Introduction

Field theories which are asymptotically free, predict that the total e^+e^- annihilation cross section into hadrons, $\sigma_{e^+e^- \rightarrow h}$ is proportional to the pure QED cross section $\sigma_{e^+e^- \rightarrow \mu^+\mu^-}$ (i.e. shows scaling) with a specified proportionality constant ⁽¹⁾ R. We feel, however, that the high momentum transfer behaviour of known electromagnetic form factors does scarcely support the idea that the interaction of the hadronic constituents is not singular at short distances. On the contrary, the proton form factors and even more the pion form factor ⁽²⁾ suggest a singular interaction ⁽³⁾. The case of asymptotically nonfree models has already been dealt with by Gribov, Joffe and Pomeranchuk ⁽⁴⁾ with qualitative arguments. Furthermore there is Wilson's short distance expansion ⁽⁵⁾, where scaling follows from the canonical dimension of the current and the existence of the unit operator. Similar arguments ⁽⁶⁾, however, for the Callan-Gross integral in deep inelastic ep-scattering, based on the energy momentum tensor, lead to the equality of the Callan-Gross integrals for neutron and proton, contrary to experience ⁽⁷⁾. Finally we want to mention the scale invariant model of Polyakov ⁽⁸⁾. There the cross section $\sigma_{e^+e^- \rightarrow \text{hadrons}}$ is described by a sum of "branching" diagrams, and scaling follows from the assumption that the sum over all diagrams introduces no extra s-dependence (s is CM-energy squared). There seems to be no control for this.

Our approach will have the same basis as that of Ref. 4. We shall consider the case where there is one (or a finite number of) fundamental spin zero fields with a local coupling to the photon. Then the total cross section $\sigma_{e^+e^- \rightarrow h}$ is given by the absorptive part of the diagram in Fig. 1, which

is the Dyson form of the complete photon self energy contribution ⁽⁹⁾ apart from a seagull term and from subtractions. The vertex and the propagators of the particle are taken as renormalized. Therefore, a cut-off dependent renormalization constant $Z_1(\Lambda^2)$ has to be included. Our first main assumption is that $Z_1(\Lambda^2)$ vanishes ⁺⁾ like a power for $\Lambda^2 \rightarrow \infty$. In this limit the absorptive part of the indicated propagators in Fig. 1 will not contribute to $\sigma_{e^+e^- \rightarrow h}$, since the integral over the loop momentum must be divergent in order to cancel $Z_1(\Lambda^2)$. This is to be contrasted with the parton model assumption ⁽¹⁰⁾ that the absorptive part of the propagators in the diagram in Fig. 2 is relevant for $\sigma_{e^+e^- \rightarrow h}$, with well-known and unpleasant consequences for the hadronic final state. Also a modified version of the parton picture ⁽¹¹⁾, namely Fig. 3, leads, if not to jets, to unwelcome constituent pairs in the final state.

For the electromagnetic vertex of the constituent field we shall use the Nakanishi spectral representation ^(12,13), which is known to hold in perturbation theory without kinematical restrictions to any momenta ⁺⁺⁾. Our physical assumption will be that the spectral weight function is as smooth as possible in its variables, being restricted primarily by $Z_1(\Lambda^2) \rightarrow 0$ for $\Lambda^2 \rightarrow \infty$. The power of the integral representation is to connect different kinematical regions in the vertex, thereby admitting the use of the Ward identity to calculate the propagators in Fig. 1 from the vertex. We shall find that a simple assumption on the spectral weight function will lead to scaling. The approach to scaling will be very slow, however, depending on the anomalous dimension of the fundamental field. Simple weight functions,

⁺⁾ This is equivalent to the required fall-off of the vertex function.

⁺⁺⁾ Contrary to the Deser-Gilbert-Sudarshan representation ^(14,12)

which take into account the power decrease of the on shell form factors, will give asymptotic values of R larger than the canonical value (which is $R(\infty) = 1/4$ for a spin zero field).

An advantage of this approach is, that there need not appear constituent pairs in the final state to an appreciable amount, as the latter is determined solely by the absorptive part of the vertex. This may conventionally be dominated by high multiplicity meson states, if the constituents are fermions. Our considerations nevertheless do not apply to a heavy quark model ⁽¹⁵⁾, as the threshold for the cross section must be in the order of the constituent mass.

There seems to be little experience how to obtain the Nakanishi spectral function for more complicated diagrams, and therefore our assumptions about its "smoothness" cannot be checked in perturbation theory. Nevertheless we think that its virtues, namely to connect $R(s)$ with on-shell and off-shell vertex functions and the propagator, deserve more attention.

In Section II we derive $R(s)$ in terms of the spectral function under the assumption $Z_4(\Lambda^2) \rightarrow 0$ for $\Lambda^2 \rightarrow \infty$. In Section III we consider special classes of spectral functions and specify the regularization scheme in terms of a cut-off in the spectral function. In Section IV we discuss generalizations and compare the approach to scaling with the trend of the experimental data.

II. Relation between $R(s)$ and the spectral function

The total cross section is given by the absorptive part of the photon propagator or, to lowest order in e^2 , by that of the photon self-energy

tensor $\Pi_{\mu\nu}$. Thus $R(s)$ can be obtained from (4)

$$\text{Im } \overline{\Pi}_{\mu\nu} = \left(-g_{\mu\nu} + \frac{q_\mu q_\nu}{s} \right) \frac{s}{12\pi} R(s) \quad (2.1)$$

where $q^2 = s$. In case of one fundamental scalar field with charge 1 one has (9)

$$\overline{\Pi}_{\mu\nu} = -i Z_1(\Lambda^2) \int \frac{d^4 k}{(2\pi)^4} \left(2k_\mu \Delta((k+\frac{q}{2})^2) \Gamma_\nu(k, q) \Delta((k-\frac{q}{2})^2) - 2g_{\mu\nu} \Delta(k^2) \right), \quad (2.2)$$

the vertex renormalization constant being given in terms of the renormalized propagator $\Delta(k^2)$ by

$$Z_1^{-1}(\Lambda^2) = -\frac{1}{\pi} \int_0^\infty d k^2 \text{Im } \Delta(k^2). \quad (2.3)$$

All quantities in (2.2) and (2.3) have to be defined by a regularization scheme depending on the cut-off parameter Λ^2 . We shall assume $\lim_{\Lambda^2 \rightarrow \infty} Z_1(\Lambda^2) = 0$, such that $\Pi_{\mu\nu}$ is of the form o times ∞ . The vertex function Γ_ν can be written as

$$\Gamma_\nu(k, q) = 2k_\nu F(s, (k-\frac{q}{2})^2, (k+\frac{q}{2})^2) + q_\nu G(s, (k-\frac{q}{2})^2, (k+\frac{q}{2})^2) \quad (2.4)$$

from which G can be eliminated by using the Ward-Takahashi identity

$$q^\nu \Gamma_\nu(k, q) = \Delta^{-1}((k+\frac{q}{2})^2) - \Delta^{-1}((k-\frac{q}{2})^2) \quad (2.5)$$

In the CMS (where $\vec{q} = 0$) we then get from (2.1) to (2.5)

$$\mathcal{R}(s) = \frac{4 Z_1(\Lambda^2)}{\pi^2 s} \text{Im} \frac{1}{i} \int d k_0 \int d \vec{k} / |\vec{k}|^4 F(s, (k-\frac{q}{2})^2, (k+\frac{q}{2})^2) \times \Delta((k-\frac{q}{2})^2) \Delta((k+\frac{q}{2})^2) \quad (2.6)$$

where the seagull term has been omitted since it is real.

In order to evaluate (2.6) we shall use the Nakanishi spectral representation ^(12,13) for F which with a suitable choice of variables reads ⁺⁾

$$F(s, (k-\frac{q}{2})^2, (k+\frac{q}{2})^2) = Z_1(\Lambda^2) + \int_0^1 d\beta \int_0^1 d\lambda \int_0^\infty d\kappa \frac{\varphi(\beta, \lambda, \kappa)}{(1-\beta)s + \beta[(1-\lambda)(k-\frac{q}{2})^2 + \lambda(k+\frac{q}{2})^2] - \kappa + i\epsilon} \quad (2.7)$$

For a given choice of the weight function φ different regions of the variables of F are connected, and therefore φ also determines the propagator Δ via the Ward identity. In the following Section the regularized φ will be specified in such a way that the assumed power behaviour of $Z_1(\Lambda^2)$ is provided. In the present Section we use (2.7) only to account for the analytic properties of F.

In order to simplify (2.6) we note that the condition $Z_1 = 0$ means that the integral diverges since $R(s)$ is finite for finite s . We first study the analytic properties of its integrand in the complex k_0 -plane. For the propagators it is clear from the Lehman spectral representation that there

⁺⁾ The usual form is $f(s_1, s_2, s_3) = \int_0^1 dz_1 \int_0^1 dz_2 \int_0^1 dz_3 \delta(1-z_1-z_2-z_3) \times \int_0^\infty d\kappa \frac{\varphi(z_1, z_2, z_3, \kappa)}{\kappa - s_1 z_1 - s_2 z_2 - s_3 z_3}$

is a pair of poles for each one of them, moving with \vec{k}^2 (and the mass), the paths starting at $\frac{\sqrt{s}}{2} \pm (m-ic)$ and $-\frac{\sqrt{s}}{2} \pm (m-ic)$ respectively as demonstrated in Fig. 4. From (2.7) it is seen that the vertex contributes a further pair of poles, the positions of which are given (in the CMS) by

$$\beta \left[\left(k_0 + (2\lambda - 1) \frac{\sqrt{s}}{2} \right)^2 - \vec{k}^2 - (1 - \lambda(1 - \lambda)) s \right] + s - k + i\epsilon = 0$$

as illustrated in Fig. 4. For $\vec{k}^2 > s - m^2$ the propagator poles no longer cross the line $\text{Re} k_0 = (1 - 2\lambda) \frac{\sqrt{s}}{2}$, and thus, for such a value of \vec{k}^2 , the Wick rotation about the point $k_0 = (1 - 2\lambda) \frac{\sqrt{s}}{2}$ no longer will pick up propagator poles. On the other hand, a value $\vec{k}^2 > s - m^2$ can be used as the lower limit of the $|\vec{k}|$ -integration without changing the result, since the contribution from below this value will vanish ^{+) for $\Lambda^2 \rightarrow \infty$ due to $Z_1(\Lambda^2)$. Now putting $k_0 = i r \omega \chi + (1 - 2\lambda) \frac{\sqrt{s}}{2}$ and $|\vec{k}| = r \sin \chi$, for large r the χ -integration can be performed and we get}

$$R(s) = \lim_{\Lambda^2 \rightarrow \infty} Z_1(\Lambda^2) \frac{3}{4\pi s} \int_{r_{\min}^2}^{\infty} dr^2 r^4 (\Delta(-r^2))^2 \text{Im} F(s, -r^2, -r^2) \quad (2.8)$$

where $r_{\min}^2 \gg |\vec{k}|_{\min}^2 > s - m^2$. It should be stressed that, since $\Delta(-r^2)$ is real, only $\text{Im} F(s, -r^2, -r^2)$ contributes.

^{+) If asymptotically the propagators behave as $(1/k^2)^{1-\delta}$ and the vertex as $(1/k^2)^\delta$ with $\delta > 0$ (see Section III) one gets $|1/k_0|^{2(2-\delta)}$ for the behaviour of the integrand which is sufficient for a finite k_0 -integration.}

For the further evaluation of (2.8) the Nakanishi representation is only needed for the special case where the denominator of (2.7) does not depend on λ which means that we can use

$$F(s, k^2, k^2) = Z_1(\Lambda^2) + \int_0^1 \beta d\beta \int_0^\infty dk \frac{f(\beta, k)}{(1-\beta)s + \beta k^2 - k + i\epsilon} \quad (2.9)$$

from which $\text{Im } F(s, -r^2, -r^2)$, and via $F(0, -r^2, -r^2)$ resp. $F(0, m^2, m^2)$ also $\Delta(-r^2)$ and $Z_1(\Lambda^2)$ can be obtained. It is to be remarked that also the on-shell form factor $F(q^2, m^2, m^2)$ is described by (2.9). In the case of $\text{Im } F(s, -r^2, -r^2)$ we get

$$\text{Im } F(s, -r^2, -r^2) = -\pi \int_0^1 \beta d\beta \theta(s - k_{\text{min}}(\beta) - (r^2 + s)\beta) \times \quad (2.10)$$

$$\times f(\beta, (1-\beta)s - r^2/\beta)$$

The form (2.10) thus determines the s -dependence of $R(s)$ and will be seen to be important for the occurrence of scaling.

III. Special Nakanishi weight functions, regularization and $R(s)$

We now have to make assumptions on the Nakanishi weight function, focussing our attention to asymptotically nonfree theories, i.e. the vertex function $F(0, k^2, k^2)$ is supposed to vanish for $k^2 \rightarrow \pm\infty$. The simplest example for this is a power law for the unregularized vertex

$$\bar{F}(0, k^2, k^2) \sim \left(\frac{1}{-k^2}\right)^\delta \quad \text{for } k^2 \rightarrow \pm\infty \quad (3.1)$$

The exponent δ gives the anomalous dimension of the propagator, which behaves as $\Delta(k^2) \sim \left(\frac{1}{-k^2}\right)^{1-\delta}$ for $k^2 \rightarrow +\infty$. We restrict ourselves to $0 < \delta < 1$.

If we write, for $\Lambda^2 = \infty$, the spectral function in (2.9) in the form

$$-\beta f_\infty(\beta, \kappa) = g(\beta, \kappa) \left(\frac{\beta}{\kappa}\right)^\delta \quad (3.2)$$

we conclude from (2.9) that the condition for (3.1) to hold is

$$0 < \left| \int_0^1 d\beta g(\beta, \infty) \right| < \infty \quad (3.3)$$

We shall consider only the special case that $g(\beta, \kappa)$ is independent of κ except for small κ , i.e. we set

$$g(\beta, \kappa) = h(\beta) \Theta(\kappa - \kappa_{\min}(\beta)) \quad (3.4)$$

The weight function of the regularized vertex depends on the somewhat arbitrary way of regularization. We shall deduce its form from that of the regularized triangle diagram Fig. 5, where the propagator of the exchanged gluon is regularized according to Pauli and Villars⁽¹⁶⁾ with a mass Λ . The weight function in (2.7) for the triangle diagram⁽¹³⁾ then gets the form, with $\Lambda \gg m$,

$$\begin{aligned} \varphi(\beta, \lambda, \kappa) = & \frac{\text{const}}{\beta^2(1-\lambda)\lambda + (1-\beta)\beta} \left[\delta\left(\kappa - (\beta^2(1-\lambda)\lambda + (1-\beta)\beta) \left(\frac{m^2}{\beta\lambda(1-\lambda)} + \frac{m^2}{1-\beta}\right)\right) \right. \\ & \left. - \delta\left(\kappa - (\beta^2(1-\lambda)\lambda + (1-\beta)\beta) \left(\frac{m^2}{\beta\lambda(1-\lambda)} + \frac{\Lambda^2}{1-\beta}\right)\right) \right] \end{aligned} \quad (3.5)$$

from which one finds that $f(\beta, \kappa) = \int_0^1 d\lambda \varphi(\beta, \lambda, \kappa)$ agrees with the unregularized function $f_\infty(\beta, \kappa)$ for $\kappa < \beta\Lambda^2$, and vanishes for $\kappa \gg \beta\Lambda^2$.

We shall replace this transition by a step function

$$f(\beta, \kappa) = f_\infty(\beta, \kappa) \Theta(\Lambda^2\beta - \kappa) \quad (3.6)$$

In the following we shall assume that (3.6) provides generally a suitable regularization scheme. We now have to express $\Delta(-k^2)$, $Z_1(\Lambda^2)$ and $\text{Im } F(s, -r^2, -r^2)$ by $f(\beta, \kappa)$, where

$$-\beta f(\beta, \kappa) = h(\beta) \left(\frac{\beta}{\kappa}\right)^\delta \Theta(\Lambda^2\beta - \kappa) \Theta(\kappa - \kappa_{\min}(\beta)) \quad (3.7)$$

Since
$$F(0, m^2, m^2) = 1 \quad (3.8)$$

independently of Λ^2 , we obtain from (2.9) in the case $\Lambda^2 \gg m^2$

$$\begin{aligned} Z_1(\Lambda^2) &\approx \int_0^1 d\beta h(\beta) \int_{\beta\Lambda^2}^\infty d\kappa \frac{\beta^\delta}{\kappa^{\delta+1}} \\ &= \frac{1}{\delta} \Lambda^{-2\delta} J \end{aligned} \quad (3.9)$$

with $J = \int_0^1 d\beta h(\beta)$. With the substitution $X = \frac{\kappa}{r^2\beta}$ (2.9) becomes in the region $r^2 \gg \kappa_{\min}$

$$\bar{F}(0, -r^2, -r^2) \approx Z_1(\Lambda^2) + J r^{-2\delta} \int_0^{\Lambda^2/r^2} dx \frac{1}{(x+1)x^\delta} \quad (3.10)$$

Then the Ward identity gives

$$\Delta^{-1}(-r^2) \approx -J \left(r^2 / \delta \Lambda^2 \delta + \int_a^{r^2} dx x^{\nu/2} x^{1-2\delta} \int_0^{\Lambda^2/r^2} dy \frac{1}{(x+1) x^\delta} \right) \quad (3.11)$$

where $\kappa_{\min} \ll a \ll r^2$.

Finally, for $\text{Im } F(s, -r^2, -r^2)$ we obtain ⁺⁾ from (2.10) with the special form (3.7)

$$\text{Im } F(s, -r^2, -r^2) = \frac{\pi s}{r^2(1+\delta)} \Theta \left(1 - \frac{\kappa_{\min}(0)}{s} - \frac{r^2}{r^2 + \Lambda^2} \right) \int_{\frac{r^2}{r^2 + \Lambda^2}}^{1 - \kappa_{\min}(0)/s} dy h \left(\frac{s}{r^2} y \right) \left(\frac{y}{1-y} \right)^\delta \quad (3.12)$$

This is valid for $r^2 \gg s \geq \kappa_{\min}(0)$. Now we put the pieces together in (2.8) and have

$$\begin{aligned} R(s) = \lim_{\Lambda^2 \rightarrow \infty} & \frac{3J}{4\delta\Lambda^2\delta} \int_{\kappa_{\min}^2}^{\infty} dr^2 r^{2(1-\delta)} \Delta^2(-r^2) \times \\ & \times \Theta \left(1 - \frac{\kappa_{\min}(0)}{s} - \frac{r^2}{r^2 + \Lambda^2} \right) \int_{\frac{r^2}{r^2 + \Lambda^2}}^{1 - \kappa_{\min}(0)/s} dy h \left(\frac{s}{r^2} y \right) \left(\frac{y}{1-y} \right)^\delta \end{aligned} \quad (3.13)$$

where $r_{\min}^2 \gg s$ (and $s \geq \kappa_{\min}(0)$) and where $\Delta^2(-r^2)$ is given by (3.11).

⁺⁾ We have made the substitution $\beta = \frac{s}{r^2 + s} y$

It is easily seen that the r -integral in (3.13) with respect to r runs effectively up to $r^2 \lesssim \Lambda^2$. Thus, since the cut-off parameter has to cancel out, and because $\Delta(-r^2)$ behaves as $(\frac{\Lambda}{r^2})^{1-\delta}$ for r^2 below Λ^2 , the second integral in (3.13) has to become a constant for $s \ll r^2 \ll \Lambda^2$. This requires

$$0 < |h(0)| < \infty \tag{3.14}$$

If (3.14) would not hold, the theory were not renormalizable. From (3.13) and (3.14) we then have

$$R(s) = \lim_{\Lambda^2 \rightarrow \infty} \frac{3 J h(0)}{4 \delta \Lambda^{2\delta}} \int_{r_{\min}^2}^{\infty} dr^2 r^{2(1-\delta)} \Delta^2(-r^2) \times \tag{3.15}$$

$$\times \Theta\left(1 - \frac{K_{\min}(0)}{s} - \frac{r^2}{r^2 + \Lambda^2}\right) \int_{\frac{r^2}{r^2 + \Lambda^2}}^{1 - K_{\min}(0)/s} dy \left(\frac{y}{1-y}\right)^\delta$$

Now (3.15) shows that for $s \gg K_{\min}(0)$ the ratio R no longer depends on s , i.e. one has scaling. Furthermore, it is seen that this constant value asymptotically is approached as $(1/s)^{1-\delta}$, i.e. with the same power with which the propagator decreases. This remarkable connection, initiated by the condition (3.14) for the finiteness of R , in terms of the spectral function means that one has the same behaviour for $\beta \rightarrow 0$ as for $K \rightarrow \infty$.

$R(s)$ has been calculated numerically since the expression (3.15) with (3.11) is a threefold integral. In Fig. 6 it is plotted for the case $h(\beta) = \text{const.}$ For other functions one has to divide these values by

$\int_0^1 d\beta h(\beta)/h(0)$ as can be verified using (3.9), (3.11) and (3.15).

It is interesting to note that qualitatively the same and quantitatively not too different results are obtained by evaluating (2.8) in a somewhat naive way. Namely, inserting (2.3) into (2.8), in the absence of a cut-off one has the quotient of two integrals diverging as functions of their upper boundaries. Assuming identical variables for these boundaries one can apply de l'Hospital's theorem to get

$$\hat{R}(s) = \frac{3}{4s} \lim_{r^2 \rightarrow \infty} \frac{r^4 \Delta^2(-r^2)}{-\text{Im} \Delta(r^2)} \text{Im} \bar{F}(s, -r^2, -r^2) \quad (3.16)$$

In the absence of a cut-off one obtains from (2.9) and (3.4) for $k^2 \rightarrow \pm\infty$

$$\bar{F}(0, k^2, k^2) \rightarrow \left(\frac{1}{-k^2}\right)^\delta \frac{\pi \mathcal{J}}{\sin \delta \pi} \quad (3.17)$$

and for $r^2 \rightarrow \infty$

$$\text{Im} F(s, -r^2, -r^2) \rightarrow \left(\frac{1}{r^2}\right)^{1+\delta} \pi s h(0) \int_0^{1 - k_{\text{min}}(0)/s} dy \left(\frac{y}{1-y}\right)^\delta \quad (3.18)$$

Then one has for $k^2 \rightarrow \pm\infty$

$$\Delta(k^2) \rightarrow - \left(\frac{1}{-k^2}\right)^{1-\delta} \frac{(1-\delta) \sin \delta \pi}{\pi \mathcal{J}} \quad (3.19)$$

Inserting (3.18) and (3.19) into (3.16) then gives

$$\hat{R}(\infty) = \frac{3h(0)}{4J} \frac{\delta(1-\delta)\pi}{\sin \delta\pi} \quad (3.20)$$

For comparison with (3.15) we note that for $h(\beta) = \text{const}$ one gets respectively from (3.20) for $\delta = 0.4$ and 0.8 the values 0.595 and 0.641 for $\hat{R}(\infty)$, which are thus about 2 to 4 times larger than the ones shown for $R(\infty)$ in Fig. 5.

Concluding this Section we remark that the basic conditions (3.3) and (3.14) for more general weight functions are replaced by

$$0 < \left| \lim_{\beta/\kappa \rightarrow 0} \beta f(\beta, \kappa) \left(\frac{\kappa}{\beta}\right)^\delta \right| < \infty \quad (3.21)$$

as the renormalizability condition. (3.21) can be obtained by introducing the expansion

$$-\beta f(\beta, \kappa) = \sum_{e, n} g_{en}(\beta, \kappa) \beta^{\delta'_e} \left(\frac{1}{\kappa}\right)^{\delta_n} \quad (3.22)$$

from which for $\delta = \text{Min } \delta_n$ and $\delta' = \text{Min } \delta'_e$ it follows that $\delta = \delta'$.

IV. Discussion

In the preceding Section we have shown that under the condition (3.4) with $h(\beta) = \text{const}$ and $\delta \approx 0.6$ one obtains an asymptotic value $R(\infty)$ close

to the pointlike value $R(\infty) = \frac{1}{4}$. The approach to scaling is, however, rather slow for this value of δ and for larger ones. For instance, for $\delta=0.6$ at $\sqrt{s}/k_{min} = 5$ only about 0.4 of the asymptotic value is reached. Before a quantitative comparison with experiment (17,18) can be made, three points have to be investigated further:

a) The assumption $h(\beta) = \text{const}$ is certainly too simpleminded.

More generally we have

$$R(s) = R(s, h(\beta) = \text{const}) \frac{h(0)}{\int_0^1 d\beta h(\beta)} \quad (4.1)$$

Now from the fact that the nucleon form factors decrease faster than $(1/Q^2)^\delta$ with $0 < \delta < 1$ for $Q^2 \rightarrow \infty$ we can deduce the following property of $h(\beta)$ without looking into specific models:

$$\int_0^1 d\beta h(\beta) \left(\frac{\beta}{1-\beta}\right)^\delta = 0 \quad (4.2)$$

If this condition would not hold, the on-shell form factor $F(q^2, m^2, m^2)$ as given by (2.9), (3.2) and (3.4) would behave as $(1/-q^2)^\delta$ for $q^2 \rightarrow +\infty$.

It should be noted that this slow fall-off, which comes from large k -contributions in (2.9), cannot be compensated by a nonasymptotic contribution in (2.9), since a finite k -interval leads at most to $F(q^2, m^2, m^2) \sim \frac{1}{q^2} \ln|q^2|$ for $q^2 \rightarrow +\infty$, if $h(1)$ is finite.

We have taken smooth functions $h(\beta)$ with one zero such that (4.2) holds.

For such functions the correction factor in (4.1) was of the order of 2 to 5. With a detailed model for the form factor one may improve such estimates in the following way. If one expands $F(-Q^2, -r^2, -r^2)$ in a power

series around $Q^2 = 0$, then for large r^2 the expansion coefficients are given by moments of $h(\beta)$, namely

$$F(-Q^2, -r^2, -r^2) = \frac{\pi}{\sin \delta\pi} \left(\frac{\kappa_0}{r^2}\right)^\delta \sum_{n=0}^{\infty} \binom{n-1+\delta}{n} \left(-\frac{Q^2}{r^2}\right)^n \int_0^1 d\beta \left(\frac{1-\beta}{\beta}\right)^n h(\beta) \quad (4.3)$$

Such an expansion may turn out to be easier to be handled than a direct calculation of the absorptive part of the vertex.

b) What is the value of $\kappa_{\min}(0)$ in realistic hadron dynamics?

Strictly speaking, from the support properties ⁽¹²⁾ of the spectral function it follows that $\kappa_{\min}(0)$ can be as low as $4m_\pi^2$ if one considers, for example, nucleons as constituents. However, more realistically one has to ask where the spectral function begins to give an appreciable contribution. Then one has to realize that the πN coupling constant $g^2/4\pi = 14$ is in effect only if the energy is large enough to overcome the baryon mass in the propagators, which in case of the annihilation diagrams in Fig. 7 means that the spectral functions essentially begins to contribute at about 1 GeV^2 . In Fig. 6 we have therefore tentatively compared the experimental results ^(17,18) using $\kappa_{\min}(0) = 1 \text{ GeV}^2$.

c) Finally one has to decide on number, charge, and spin of the fundamental constituents. Conservatively one may work with 4 charged fermions ($p, \Sigma^+, \Sigma^-, \Xi^0$) and 2 charged bosons (π^+, K^+). This multiplies our curves in Fig. 6, including the correction factor of a) and a factor 4 for spin $\frac{1}{2}$, by a factor of about 30 to 90. Thus, dividing the experimental

results ^(17,18) by 50 is reasonable for a tentative comparison in Fig. 6. It is seen that the data come close to the curve for $\delta = 0.6$.

An important result was that, due to the $Z_1 = 0$ condition, no contributions from the constituent legs in Fig. 1, i.e. no jets occur. Applying this condition now to the relation between vertex and off-shell scattering amplitude in Fig. 8 one similarly concludes that the absorptive part of the vertex is given by the absorptive part of the off-shell scattering amplitude. The main contributions to the latter may be those from the low mass high multiplicity meson exchanges and not from baryon-antibaryon intermediate states since incoming constituent baryons are infinitely far from the mass shell.

It is to be noted that the constituents in Fig. 1 cannot be massive quarks with $M^2 \rightarrow \infty$ since for each $\beta > 0$ with $h(\beta) \neq 0$ the cut of the propagator starts at $\text{Min}\left(\frac{\kappa_{\text{min}}(\beta)}{\beta}\right)$, and on the other hand, it has to do so above the particle mass. Thus, for fixed s with $\kappa_{\text{min}} \sim M^2$ the cross section vanishes.

Acknowledgements

The authors are indebted to K. Symanzik for a stimulating discussion. One of us (W.K.) wishes to express his gratitude to H. Joos, H. Schopper, K. Symanzik and G. Weber for the kind hospitality extended to him at DESY.

References

- 1) T. Appelquist and H. Georgi, Phys. Rev. D8 (1973) 4000;
A. Zee, Phys. Rev. D8 (1973) 4038.
- 2) C.J. Bebek et al., Phys. Rev. D9 (1974) 1229.
- 3) S.D. Drell and T.D. Lee, Phys. Rev. D5 (1972) 1738.
- 4) V.N. Gribov, B.L. Joffe and I. Ya. Pomeranchuk,
Phys. Lett. 24B (1967) 554.
- 5) K. Wilson, p. 116 in "Proceedings of the 1971 International
Symposium on Electron and Photon Interactions at High Energies",
edited by N.B. Mistry (Cornell Univ. Press, Ithaca, N.Y., 1972);
Phys. Rev. 179 (1969) 1499.
- 6) G. Mack, Phys. Rev. Lett. 25 (1970) 400.
- 7) E.D. Bloom, p. 227 in "Proceedings of the 6th International Symposium
on Electron and Photon Interactions at High Energies", 1973, edited by
H. Rollnik and W. Pfeil (North-Holland Publ. Comp., Amsterdam - London 1974).
- 8) A.M. Polyakov, Zh. Exp. Theor. Fiz. 59 (1970) 542.
- 9) J.D. Bjorken and S.D. Drell, Relativistic Quantum Fields
(Mc Graw-Hill, Inc., New York, 1965).
- 10) N. Cabibbo, G. Parisi and M. Testa, Nuovo Cim. Lett. 4 (1970) 35
- 11) M.S. Chanowitz and S.D. Drell, Phys. Rev. Lett. 30 (1973) 807, and
Phys. Rev. D9 (1974) 2078.
- 12) N. Nakanishi, Graph Theory and Feynman Integrals
(Gordon and Breach, New York, 1971)

- 13) N. Nakanishi, Prog. Theor. Phys. Suppl. 18 (1961) 1.
- 14) S. Deser, W. Gilbert, and E.C.G. Sudarshan, Phys. Rev. 115 (1959) 731.
- 15) M. Böhm, H. Joos and M. Krammer, Acta Phys. Austriaca Suppl. XI
(1973) 3 (Schladming Lectures 1973);
G. Preparata, Phys. Rev. D7 (1973) 2973.
- 16) W. Pauli and F. Villars, Rev. Mod. Phys. 21 (1949) 434.
- 17) G. Tarnopolsky et al., Phys. Rev. Lett. 32 (1974) 432.
- 18) J.-E. Augustin et al., SLAC-LBL-preprint, Jan. 1975

Figure Captions

Fig. 1: Photon self energy diagram

Fig. 2: Diagram leading to the parton model

Fig. 3: Modified parton model diagram

Fig. 4: Path of the propagator and vertex poles in the complex k_0 -plane. Units are $\sqrt{s}/2$.

Fig. 5: Triangle diagram. The gluon propagator to be regularized is denoted by G.

Fig. 6: $R(s)$ for one spin zero constituent and for $h(\beta) = \text{const.}$
x CEA results ⁽¹⁷⁾ times 0.02.
+ SPEAR results ⁽¹⁸⁾ times 0.02.

Fig. 7: Baryon annihilation diagrams with multi meson exchanges.
The propagators are dressed ones.

Fig. 8: Equation relating vertex and off-shell scattering amplitude.

Z_1

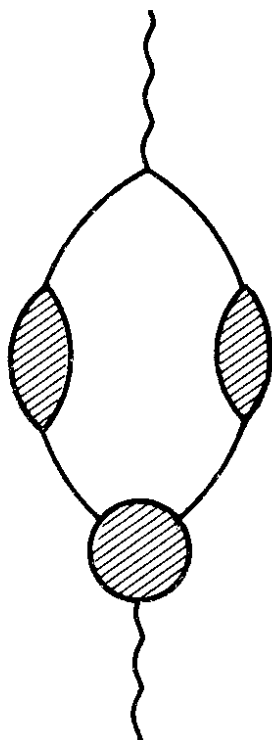


Fig.1

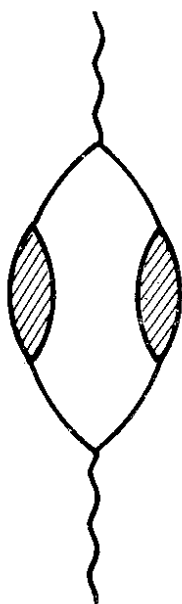


Fig.2

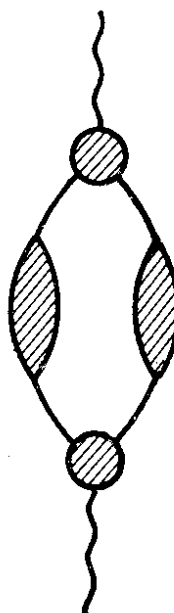


Fig.3

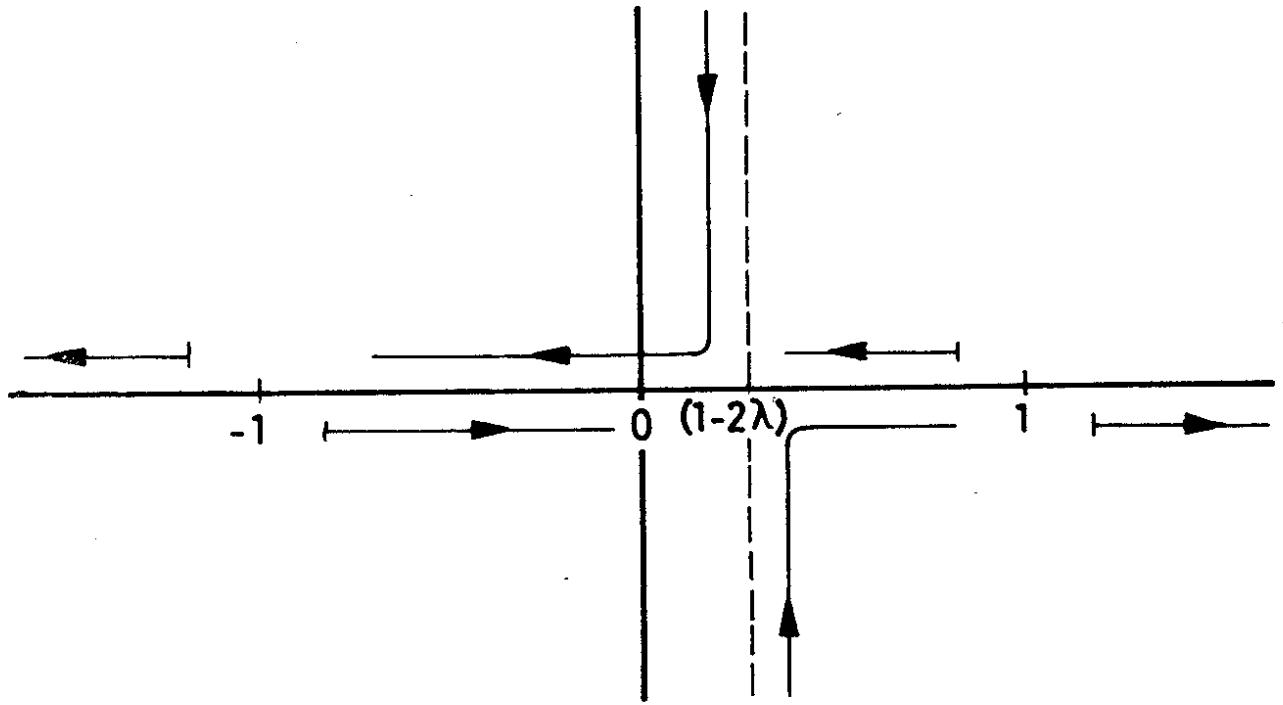


Fig.4

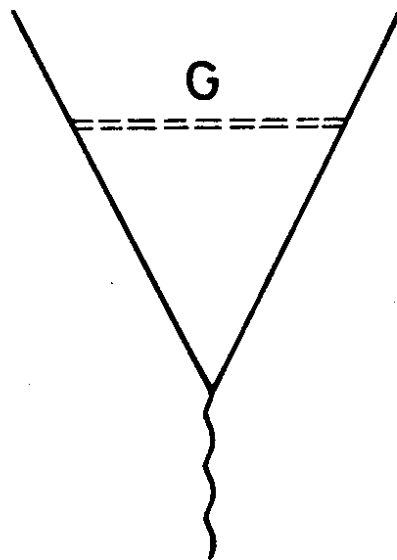


Fig.5

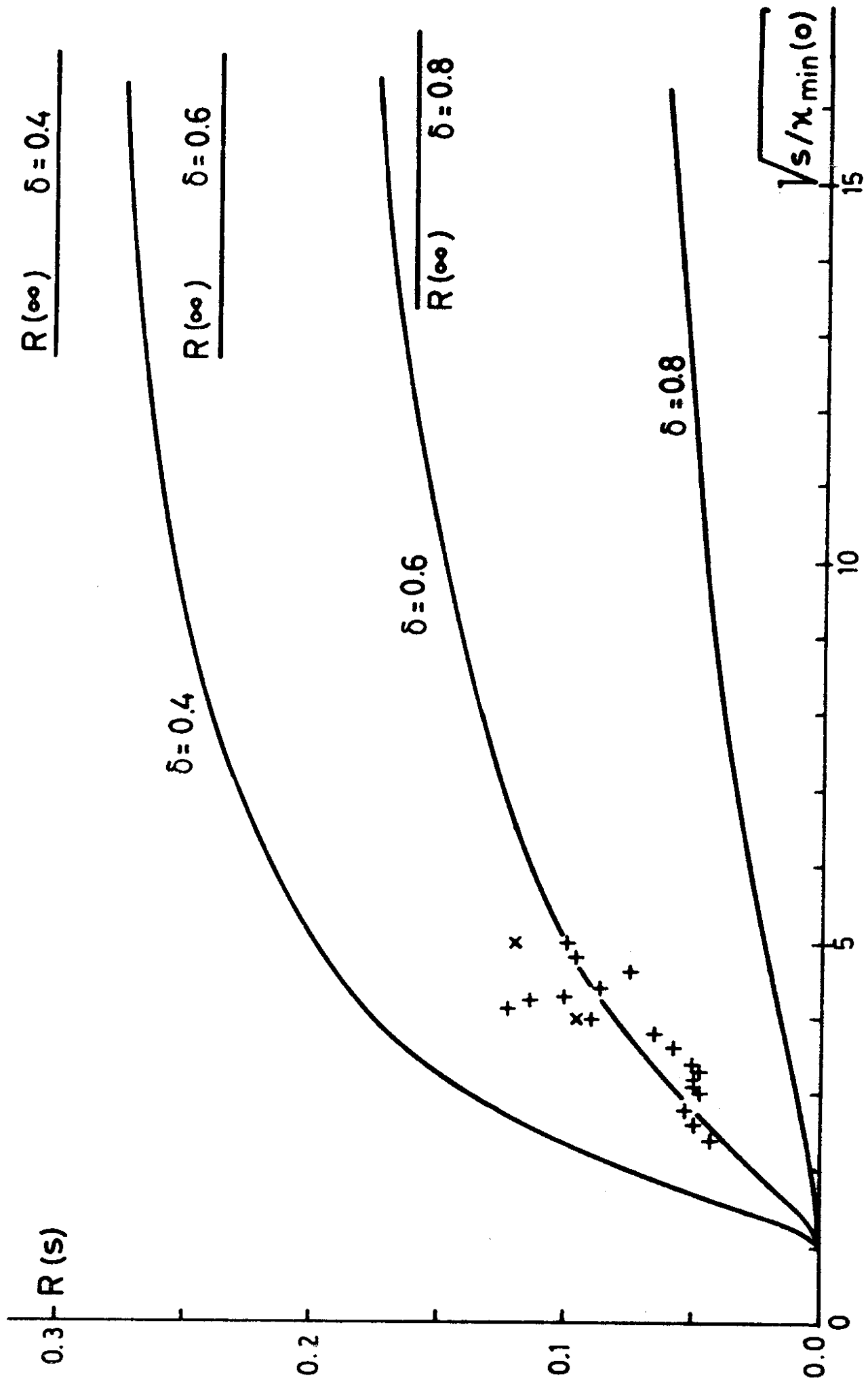


Fig. 6

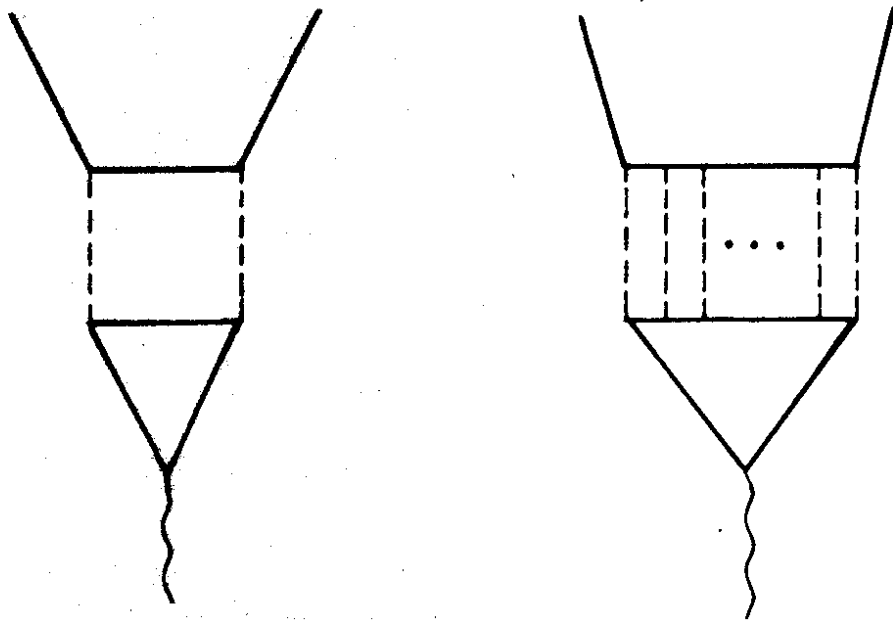


Fig.7

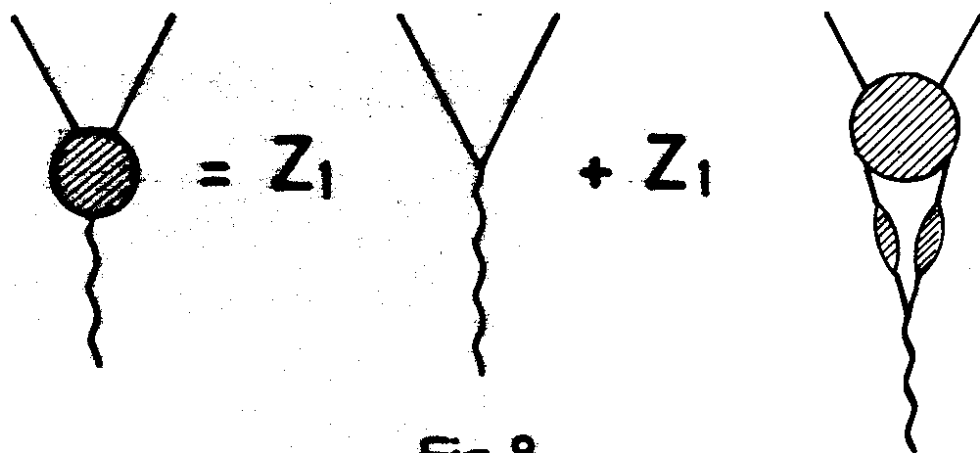


Fig.8